CrossMark

Analysis of the expression of human bitter taste receptors in extraoral tissues

Appalaraju Jaggupilli[1,2] · Nisha Singh[1,2] · Jasbir Upadhyaya[1,2] · Anurag S. Sikarwar[1,2] ·
Makoto Arakawa[1,2,3] · Shyamala Dakshinamurti[1,4,5] · Rajinder P. Bhullar[1,2] ·
Kangmin Duan[1,2,5] · Prashen Chelikani[1,2,5,6]

Abstract The 25 bitter taste receptors (T2Rs) in humans perform a chemosensory function. However, very little is known about the level of expression of these receptors in different tissues. In this study, using nCounter gene expression we analyzed the expression patterns of human TAS2R transcripts in cystic fibrosis bronchial epithelial (CuFi-1), normal bronchial epithelial (NuLi-1), airway smooth muscle (ASM), pulmonary artery smooth muscle (PASM), mammary epithelial, and breast cancer cells. Our results suggest a specific pattern of TAS2R expression with TAS2R3, 4, 5, 10, 13, 19, and 50 transcripts expressed at moderate levels and TAS2R14 and TAS2R20 (or TASR49) at high levels in the various tissues analyzed. This pattern of expression is mostly independent of tissue origin and the pathological state, except in cancer cells. To elucidate the expression at the protein level, we pursued flow cytometry analysis of select T2Rs from CuFi-1 and NuLi-1 cells. The expression levels observed at the gene level by nCounter analysis correlate with the protein levels for the T2Rs analyzed. Next, to assess the functionality of the expressed T2Rs in these cells, we pursued functional assays measuring intracellular calcium mobilization after stimulation with the bitter compound quinine. Using PLC inhibitor, U-73122, we show that the calcium mobilized in these cells predominantly takes place through the Quinine–T2R–Gαβγ–PLC pathway. This report will accelerate studies aimed at analyzing the pathophysiological function of T2Rs in different extraoral tissues.

✉ Prashen Chelikani
Prashen.Chelikani@umanitoba.ca

[1] Manitoba Chemosensory Biology (MCSB) Research Group, University of Manitoba, Winnipeg, MB R3E 0W4, Canada

[2] Department of Oral Biology, University of Manitoba, Winnipeg, MB R3E 0W4, Canada

[3] Department of Dental Hygiene, Chiba Prefectural University of Health Sciences, Winnipeg, Canada

[4] Departments of Pediatrics, Physiology, University of Manitoba, Winnipeg, Canada

[5] Biology of Breathing, Children's Hospital Research Institute of Manitoba (CHRIM), Winnipeg, Canada

[6] Department of Pharmacology and Therapeutics, University of Manitoba, Winnipeg, MB R3E 0W4, Canada

Introduction

Bitter taste receptors (T2Rs) belong to the G protein-coupled receptor (GPCR) superfamily. In humans, there are 25 T2Rs which are distinct from other classes of GPCRs and considered as a separate group [1]. T2Rs are known for their primary role in bitter taste perception, one of the five basic taste modalities in mammals [2]. The nomenclature was based on their initial discovery in the oral cavity and for their vital role in the evaluation of quality and nutritious value of food [2, 3]. T2Rs were also discovered in the gut and were suggested to have evolved as a central warning signal to induce aversion towards noxious or harmful substances [4].

🖄 Springer

Several recent studies have demonstrated the expression of T2Rs in extraoral tissues in different model systems reviewed in [5]. T2Rs were suggested to exhibit distinct functions with respect to the tissue in which they are expressed. The initial evidence for extraoral expression of taste receptors came from the discovery of α-gustducin in the gut [6]. Following these studies, the expression of T2Rs was shown in the gastrointestinal (GI) tract where they function in sensing luminal contents and GI hormones [4]. Successive investigations have expanded the expression and function of T2Rs to the detection of bacterial stimulants in upper airways, bronchodilation in lower airways, vasoconstriction in vasculature, nutrient sensing in heart, spermatogenesis in testis, regulation of thyroid-stimulating hormone (TSH)-dependent functions in thyroid, anti-inflammation and sensing quorum-sensing molecules in immune system, and keratinocyte differentiation in skin [7–15]. Despite the reports on the expression of functional T2Rs in brain, breast cancer, and bone marrow cells, their exact role in these tissues remains to be elucidated [16–18].

T2Rs like most other GPCRs are endogenously expressed at very low levels. The expression and distribution (or number) of T2Rs varies considerably among different tissues. Most of the previous studies employed RT-PCR, qPCR and microarray techniques to analyze the gene expression of TAS2Rs [19]. These techniques that require library preparation and/or pre-amplification can introduce bias in the results [20]. In general, the expression levels of genes and the proteins they code might vary in different tissues, depending on a number of physiological conditions. Our hypothesis is that T2Rs might be differentially expressed in different extraoral tissues and in normal versus pathophysiological conditions. To test this hypothesis, in this study we used state-of-the-art nCounter gene expression analysis to characterize the expression of the 25 human TAS2Rs in different tissues including cell lines from pathological conditions. Our results suggest a specific pattern of TAS2R expression with TAS2R7, 16, 38, 39, 40, 41, and 42 at barely detectable levels, TAS2R1, 8, 9, and 60 at low levels, TAS2R3, 4, 5, 10, 13, 19, and 50 at moderate levels, and TAS2R14 and TAS2R20 (or TAS2R49) at high levels. This pattern of expression is mostly independent of tissue origin and the pathological state, except in breast cancer cells.

Next, we analyzed the protein expression of select T2Rs in CuFi-1 and NuLi-1 airway cells by flow cytometry. To test the T2R signaling pathway, we treated NuLi-1 and CuFi-1 cells with U-73122 (PLC inhibitor) and measured their activation by the bitter ligand, quinine. Treatment with U-73122 caused a dramatic inhibition of quinine-mediated intracellular calcium response. This suggests that majority of the intracellular calcium mobilized in these cells upon quinine treatment is due to the activation of T2Rs.

Materials and methods

Materials

Cell culture media and culture supplements were purchased from Invitrogen and ThermoFisher Scientific (Burlington, ON, Canada), Lonza, and Cedarlane (Burlington, ON, Canada). RNA isolation kit and cDNA synthesis kit were purchased from Qiagen (Toronto, ON, Canada) and Invitrogen. The nCounter CodeSets for TAS2Rs and the tissue markers were purchased from NanoString Technologies (Seattle, WA, USA). The HUGO gene nomenclature is used wherever the genes are mentioned. The polyclonal antibodies for flow cytometry analysis are rabbit anti-T2R3 (OAAF05229) and rabbit anti-T2R5 (OASG06985) purchased from Aviva Systems Biology (San Diego, CA, USA), rabbit anti-T2R4 (OSR00153 W, whole serum) from Thermo Scientific (Burlington, ON, Canada), rabbit anti-T2R10 (sc-169473), goat anti-T2R20 (T2R49) (sc-34531), goat anti-T2R38 (sc-34294) purchased from Santa Cruz Biotechnology (Dallas, TX, USA), and mouse anti-β_2AR monoclonal antibody (MCA2784) purchased from Bio-Rad (Mississauga, ON, Canada). Isotype controls such as normal rabbit serum (sc-2338), normal rabbit IgG (sc-3888), normal mouse IgG (12-371), and normal goat IgG (sc-3887) were purchased from Santa Cruz Biotechnology. The phospholipase C inhibitor (U-73122) and quinine hydrochloride were purchased from Sigma-Aldrich (Toronto, ON, Canada).

Cell culture

Human bronchial epithelial cells from normal lung with immortalized E6/E7 and hTERT expression (NuLi-1, CRL-4011) and human airway epithelial cells from a cystic fibrosis (CF) patient homozygous for ΔF508/ΔF508 and immortalized with E6/E7 and hTERT expression (CuFi-1, CRL-4013) were purchased from ATCC. The cells were grown in cell culture plates coated with human placental collagen type IV as recommended by ATCC and maintained in serum-free bronchial epithelial cell growth medium from Lonza (BEGM Bullet Kit; CC-3170). Human mammary epithelial cell line MCF-10A and the highly invasive breast cancer cell line MDA-MB-231 were kind gifts from Dr. James Davie and Dr. Etienne Leygue, Research Institute in Oncology and Hematology, Winnipeg, Canada. MCF-10A cells were maintained in DMEM supplemented with 5% horse

serum, hydrocortisone (0.5 µg/ml), insulin (10 µg/ml), epidermal growth factor (20 ng/ml), and penicillin–streptomycin (100 µg/ml each). MDA-MB-231 cells were cultured in DMEM supplemented with 10% serum. Human pulmonary artery smooth muscle cells (hPASMCs) were purchased from ATCC, and human airway smooth muscle cells (hASMCs) were a kind gift from Dr. Andrew Halayko, Biology of Breathing, Children's Hospital Research Institute of Manitoba. hPASMCs were grown in a vascular cell basal medium supplemented with hPASMC growth kit [10]. hASMCs were grown in DMEM supplemented with 10% serum. All cells were maintained in an incubator at 37 °C supplied with 5% CO_2.

mRNA preparation

Total RNA from the cells was isolated according to the manufacturer's instructions using the RNeasy Mini kit (Qiagen, Canada). The concentration and purity of the RNA were determined using a NanoDrop 2000 (ThermoFisher Scientific, Canada).

nCounter gene expression analysis

nCounter sequencing was performed at the Farncombe Metagenomics Facility, McMaster University, Canada. All the procedures were performed according to the recommendations from NanoString technologies. The quality of extracted mRNA was analyzed by a BioAnalyzer, and based on the RNA integrity number and the 28S/18S ratios, only intact RNA of good quality was used in nCounter sequencing and data analysis. From each sample, 100 ng of RNA was hybridized to the custom-designed CodeSets sequences. The details of the CodeSets are shown in Table 1. Six synthetic positive control templates and the corresponding probes are built into the CodeSets by NanoString technologies. The positive controls are used to confirm that the hybridization worked and to normalize for technical variation. Eight negative control probes were also built into the CodeSet by NanoString technologies, but there was no matching template sequence added for them to bind to and these are used to monitor background-level hybridization. Data analysis was performed using the nSolver™ 2.0 analysis software (NanoString technologies). The geometric mean of negative controls was used for background subtraction. This was followed by positive control normalization where the raw counts were normalized using the geometric mean of the 6 positive control probes provided in the probe set. The data are represented as nCounter values. One count of the nCounter value can be interpreted as one mRNA transcript in 100 ng of RNA.

Analysis of cell surface expression of T2Rs by Fluorescence-Activated Cell Sorter (FACS)

FACS analysis of selected T2Rs was performed on NuLi-1 and CuFi-1 cell lines using BD FACS Canto machine as described previously [17]. 50,000 viable cells were collected for the experiment and washed 2–3 times with FACS buffer containing 0.5% BSA in PBS and stained with primary anti-T2R polyclonal antibodies at 1:200 dilution for T2R3 and T2R5, 1:300 for T2R4, T2R10, T2R20 (T2R49), and T2R38, and monoclonal antibody at 1:25 dilution for β_2AR (positive control). Appropriate rabbit serum, rabbit IgG, or goat IgG were used as isotype controls, and only cells were kept as negative controls and incubated on ice for 1 h. Subsequently, the cells were washed with FACS buffer and incubated with the respective secondary antibody conjugated with Alexa Fluor-488 (1:1000) in dark on ice for 1 h. The cells were washed and then resuspended in 300 µl FACS buffer for analysis. 10,000 events were collected and the results were analyzed using FACS Diva or FlowJo software. The mean fluorescence intensity (MFI) values of isotype controls were subtracted to analyze protein expression.

Calcium mobilization assay

Calcium mobilization assays were performed as described earlier [17]. NuLi-1 and CuFi-1 cells (0.5×10^5) were plated in a collagen-coated 96-well black-walled BD Optilux plate and incubated in 5% CO_2 incubator for 24 h. Briefly, concentration-dependent changes in intracellular calcium induced by the bitter compound quinine in NuLi-1 and CuFi-1 cells and the same cells treated with the PLC inhibitor, U-73122 (5 µM for 30 min prior to quinine addition), were measured. Changes in intracellular calcium mobilized as detected by calcium-sensitive dye Fluo 4NW (Invitrogen) were measured in RFUs. Data represent four independent experiments with each data point in triplicate. EC_{50} values were calculated using GraphPad PRISM software.

Results and discussion

The T2R subfamily with 25 TAS2Rs are next only to olfactory and adhesion receptors in numerical strength among the ~ 700 GPCRs in humans. In this study, we used the state-of-the-art gene sequencing technique, the nCounter platform, to analyze the expression of the 25 TAS2Rs. This technique is based on the hybridization of complementary probe sequences spanning 100 nucleotide bases for each gene. Thus, it made it difficult to design specific probes or CodeSets for TAS2Rs 30, 31, 43, 45, and

Table 1 CodeSet design of TAS2Rs for the nCounter gene expression analysis

Sl. no.	Gene	Nanostring ID	PubMed Accession	Targeted region	Target sequence
1	TAS2R1	NM_019599.2:1228	NM_019599.2	1229–1328	TGGATCAGTTCAAAGAACCCATGATTCAAATG ATTTACCCATGCTGCCACACTTC CCTCAGCCAGACAAAGCAGCCTGTTCATAAAT ATACAAACATGTCC
2	TAS2R3	NM_016943.2:458	NM_016943.2	459–558	ATGCTGTTGGGTGCACTGCTCTTATCCTGTGGT AGTACCGCATCTCTGATCAATGAGTTTAA GCTCTATTCTGTCTTTAGGGGAATTGAGGCCACCAGGA
3	TAS2R4	NM_016944.1:272	NM_016944.1	273–372	GGACTCGAGCAGTGTCTGCTTGTTGTGAC CTTGCTCAATATCTTGTACTGTG TGAAGATTACTAACTTCCAACACTCAGTGTTTCT CCTGCTGAAGCGGAAT
4	TAS2R5	NM_018980.2:248	NM_018980.2	249–348	GGATCAGAAAATTCAACTGGTCCTCATATAACC TCATTATCCTGGCCTGGCTGGCCTGCGATTTCTCCTGCA GTGGCTGATCATTTTGGACTTAAGCTT
5	TAS2R7	NM_023919.2:450	NM_023919.2	451–550	TGGATTCTACTGGGGTGCGTGGTTCTCTCTGTGTT TATTAGCCTTCCAGCCACTGAGAATTTGAACGCTGATTTC AGGTTTTGTGTGAAGGCAAAGAGGA
6	TAS2R8	NM_023918.1:350	NM_023918.1	351–450	ACTTTTTCTCTGGCTGAAGTGGAAAATTGATATGGTGGTGC ACTGGATCCTGCTGGGATGCTTTGCCATTTCCTTGT TGGTCAGCCTTATAGCAGCAATA
7	TAS2R9	NM_023917.2:772	NM_023917.2	773–872	ACATGAGGGCCATAAAGGCAGTGATCATCTTTCTGCTCCTC CTCATCGTGTACTACCCAGTCTTTCTTGTTAT GACCTCTAGCGCTCTGATTCCTCAGGG
8	TAS2R10	NM_023921.1:586	NM_023921.1	587–686	TAATCATTTCCCTTTGGAGACACAACAGGCAGATGC AATCGAATGTGACAGGATTGAGAGACTCCAACAC AGAAGCTCATGTGAAGGCAATGAAAGTTTT
9	TAS2R13	NM_023920.2:1036	NM_023920.2	1037–1136	AGAACACAGTGATCTACATGCTTTGTGAGAC GATTGGAGTCTTCTCTCCTCCAAGCCACTCCTT TCTTCTGATTCTAGGAAACGCTAAGTTAAGACAGGC
10	TAS2R14	NM_023922.1:818	NM_023922.1	819–918	TTCATGTCACTCATGTGTTCTGATTCTTGGAAA CAAGAAGCTGAGACAGGCCTCTGTCGTGC TACTGTGGCTGAGGTACATGTTCAAAGATGGGGAG
11	TAS2R16	NM_016945.2:370	NM_016945.2	371–470	TCTACTGCATCAAGGTCTCTTCTTTCACCCAT CACATCTTTCTGCTGGCTGAGGTGGAGAATTTTGAGGTTGT TTCCCTGGATATTACTGGGTTCTCTGAT
12	TAS2R19 (TAS2R48)	NM_176888.1:768	NM_176888.1	769–868	AGCAAACTTGTACTCCTGCTTTGCCAAACT GTTGCAAATCATGTATCCTTCATTCCACTC ATTCATCCTGATTATGGGAAGTAGGAAGCTAAAACAGACCT
13	TAS2R20 (TAS2R49)	NM_176889.2:443	NM_176889.2	444–543	CACGTATATAAAATGTGTGGACAGAAGAATG TGAAGGAAACGTAACTTGGAAGATCAAA CTGAGGAATGCAATGCACCTTTCCAACTTGACTGTGAGCCATG

Table 1 continued

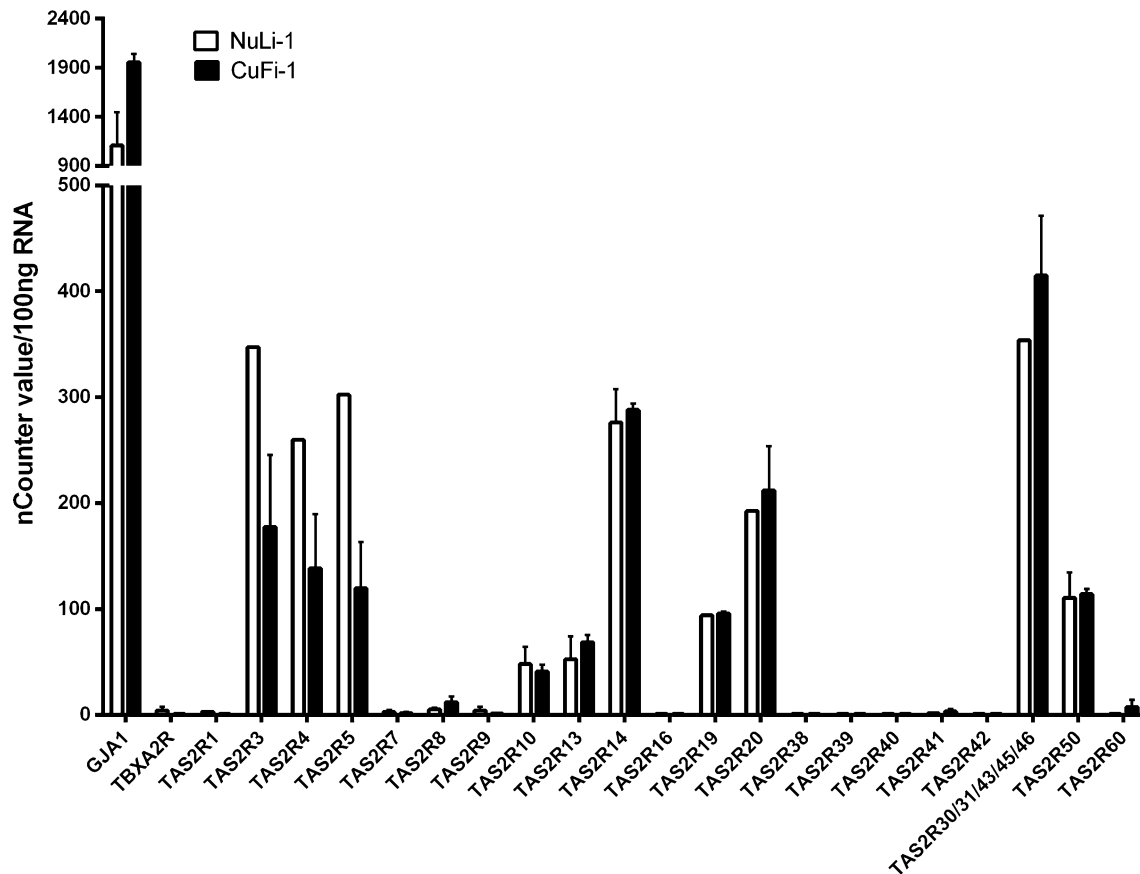| Sl. no.	Gene	Nanostring ID	PubMed Accession	Targeted region	Target sequence
14	TAS2R38	NM_176817.4:446	NM_176817.4	447–546	CATCCGTTCTCTCACACCTTCCTGATCT GCTTGGCAAGCTGGGTCTCCAGGAAGATC TCCCAGATGCTCCTGGGTATTATTCTTTGCTCCTGCATCTGC
15	TAS2R39	NM_176881.2:564	NM_176881.2	565–664	CCTATCCACTCCTCCAACTCCACTAA GAAAACATACTTGTCTGAGATCAATGTGGTC GGTCTGGCTTTTTCTTTAACCTGGGGATTGTGACTCCTCTGA
16	TAS2R40	NM_176882.1:50	NM_176882.1	51–150	GGTCACCTTCACTTTGGTGTCTCCGGAATA GAGTGCATCACTGGCATCCTTGGGAGTGGCT TCATCCACGGCCATCTATGGGCTGAGTGGGCCAGGGGC
17	TAS2R41	NM_176883.2:759	NM_176883.2	760–859	GCCGCAAAATTTATCTCCATGCAGAACGACTT TTACTGGCCATGGCAAATTGCAGTCTACCTG TGCATATCTGTCCATCCCTTCATCCTCATCTTCAGCA
18	TAS2R42	NM_181429.1:202	NM_181429.1	203–302	TAGTGGGACTTGCTTCACATTTATATACCACAT ATAGACTAGGAAAAACTGTTATTATGC TTTGGCACATGACTAATCACTTGACAACCTGGCTTGCCAC
19	TAS2R30/31/43/45/46	NM_176884.2:820	NM_176884.2	821–920	TGATATCAGTTTGGAGTTTTGGAAGTC TGGAAAACAAACCTGTCTTCATGTTCTGCAAAGC TATTAGATTCAGCTATCCTTCAATCCACCCATTCATCCT
20	TAS2R50	NM_176890.2:479	NM_176890.2	480–579	ATCTTCTTGTGGCAAACATGGATGA GAGTATGTGGGCAGAAGAATATGAAGGAAACATGACTGGG AAGATGAAATTGAGGAATACAGTACATCTTTCATA
21	TAS2R60	NM_177437.1:76	NM_177437.1	77–176	TTTTACGCCTGGTAGCAATAGCAGGCA ATGGCTTCATCACTGCTGCT CTGGGCGTGGAGTGGGTGCTACGGAGAATGTTGTTGCC TTGTGATAAGTTATT
22	GJA1	NM_000165.3:705	NM_000165.3	706–805	GCGAACCTACATCATCAGTATCCTCTT CAAGTCTATCTTTGAGGTGGC CTTCTTGCTGATCCAGTGGTACATCTATGGATTCAGCTTG AGTGCTGTTTAC
23	TBXA2R (TxA2)	NM_001060.3:385	NM_001060.3	386–485	CACACGCGCTCCTCCTTCCTCCACCTTCCTCGCGGCCTCGTCCTC ACCGACTTCCTGGGCGTGCTGGTGACCGGTACCATC GTGGTGTCCCAGCACGCCG
24	ESR1	NM_000125.2:2390	NM_000125.2	2391–2490	TGCTATGTTACTAAGCGTGAGGATTCCCGTAGCTCTTCACAGC TGAACTCAGTCTATGGGTTGGGGCTCAGATAACTCTGTGC ATTTAAGCTACTTGTAG

Fig. 1 The mRNA expression levels of TAS2Rs in NuLi-1 and CuFi-1 cells. The nCounter analysis was performed as described in the "Methods" section. nCounter values were represented on the *Y* axis and the genes analyzed on the *X* axis. One count of the nCounter value can be interpreted as one mRNA transcript in 100 ng of total RNA. Connexin-43 (GJA1) gene was included as an epithelial cell marker and the gene for the vasoconstrictor receptor, thromboxane A_2 receptor (TBXA2R), was used as an additional reference. Results presented are from two independent preparations and all values shown represent the average value. No significant difference in the expression of TAS2Rs was observed between the two cell lines

46 which share a high degree of sequence similarity of >92% (Fig. S1, supplementary material). The designed CodeSets could not differentiate between these five TAS2Rs (Table 1). Therefore, wherever listed, the nCounter value represents the total expression of those five TAS2Rs. Nevertheless, the nCounter sequencing technique has many advantages. It allows multiplexed measurement of mRNA transcripts in a single reaction without the requirement for reverse transcription and pre-amplification for analysis of 100 ng or more of nucleic acid target. nCounter sequencing utilizes molecular barcodes that enable direct digital detection of individual mRNA transcripts [21].

NuLi-1 and CuFi-1 cells are immortalized bronchial epithelial cell lines derived from a normal and a cystic fibrosis patient, respectively. The nCounter gene expression analysis showed no statistically significant differences in TAS2R expression between these two cell types (Fig. 1). Based on the nCounter values, TAS2R14 and 20 (or 49) showed higher expression levels, followed by TAS2R3, 4, 5, 50 and then TAS2R10, 13, and 19. The other TAS2Rs showed very low or barely detectable expression. Next, we pursued characterizing TAS2R expression in normal mammary epithelial cell line MCF-10A, the highly invasive breast cancer cell line MDA-MB-231, and in hASMCs and hPASMCs (Figs. 2, 3). As observed in the case of NuLi-1 and CuFi-1, the expression patterns of the different TAS2Rs were similar. However, the mammary epithelial cell lines showed statistically significant difference in expression between the normal and cancerous cell lines for TAS2R14 and 20 (or 49), the two highly expressed TAS2Rs (Fig. 2). Although TAS2R30/31/43/45/46 showed statistically significant differential expression between the cell lines, given the ambiguity with the CodeSet for these five TAS2Rs, their individual transcript levels could not be confirmed. In smooth muscle cells from airways and pulmonary artery, similar TAS2R expression pattern was observed, which correlates with PCR and microarray data
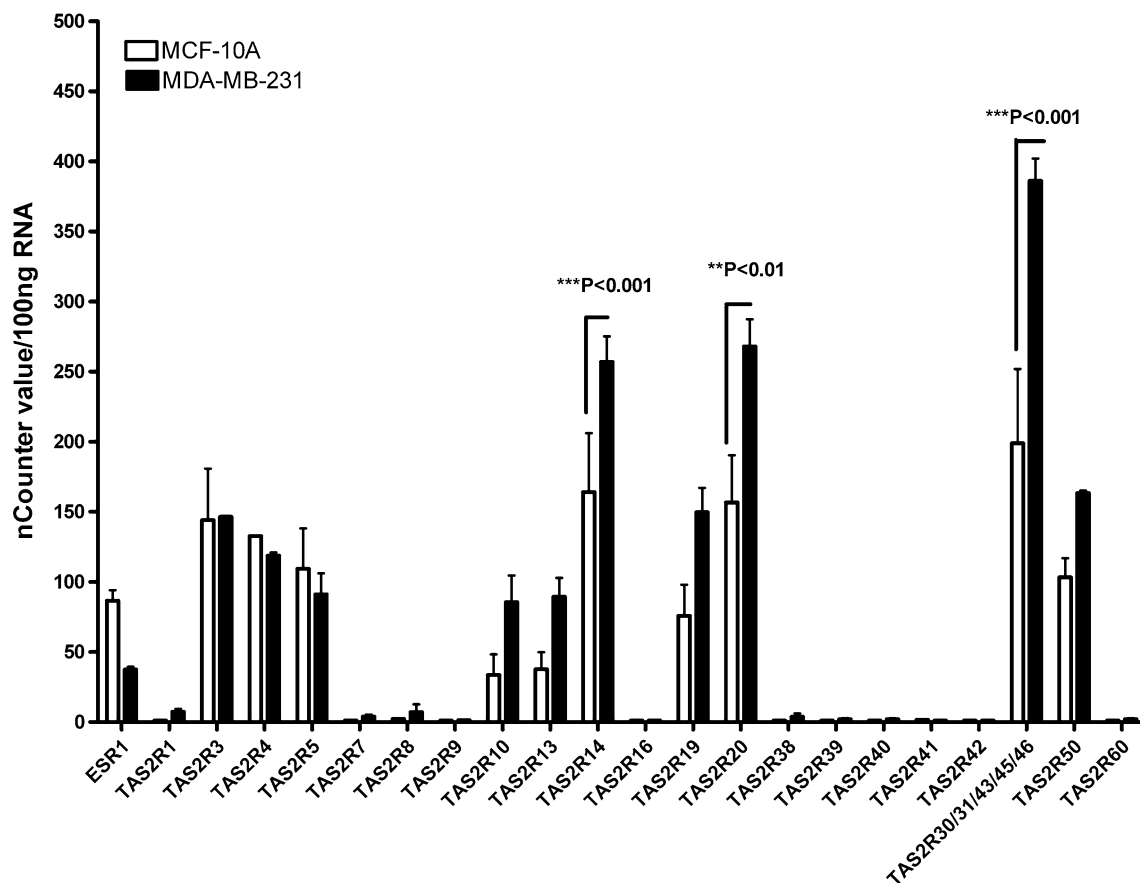
Fig. 2 The mRNA expression levels of TAS2R genes in normal breast epithelial cells MCF-10A and in highly invasive breast cancer cells MDA-MB-231. The MDA-MB-231 cell line is estrogen receptor (ESR1) negative, and ESR1 was used as a control gene. nCounter values were represented on the *Y* axis and the genes analyzed were on the *X* axis. The expression of TAS2R14 and 20 showed a significant difference between MCF-10A and MDA-MB-231. Data presented are from two independent experiments and the values are plotted as mean ± SEM. The results were analyzed using two-way ANOVA. Statistically significant values are shown by *asterisk*

for these cells from previous studies [10, 18, 22]. These earlier analysis in ASMCs showed a similar pattern of expression for most of the TAS2Rs except TAS2R10 being more abundant than TAS2R14 followed by TAS2R31, which were termed as 'high expressors' with respect to the expression of ADRB2 [22]. The other TAS2Rs (TAS2R3, 4, 5, 19, 20, 45, 50, 30, 9, 13, 42, 46, 1, and 8) were considered as modest and the rest as low expressors. Moreover, the levels of expression of these TAS2Rs correlate with the receptor function in response to their respective agonists.

It is unclear whether pathological conditions influence the expression or regulation of TAS2Rs. In previous studies, qPCR analysis on healthy and diseased human heart tissues showed a similar pattern of TAS2R transcript expression [11, 23]. In one of these studies, an in silico analysis was also performed and no relative changes were demonstrated in both healthy and diseased hearts [23]. Another evidence for this paradigm was also observed between asthmatic and non-asthmatic hASMCs [24]. Our

data that suggest no differential expression of TAS2Rs in CF vs. non-CF airway cell lines are in agreement with those reported in these studies. Interestingly, the TAS2R expression in cancer cells seems to go against this pattern. Given the nature of changes that take place in a cancerous cell, these cells are expected to undergo significant alterations in morphological and mechanistic characteristics compared to a normal cell. This might explain the observed differential expression of TAS2Rs in MCF10A and MDA-MB-231 cells (Fig. 2). Connections between bitter taste compounds and cancer have been studied before. For instance, increasing coffee consumption lowers the risk of hepatic carcinoma and the bitter compound cromolyn reduces the risk of pancreatic cancer [25]. Likewise, bitter compounds like lupulones from hops or epigallocatechin gallate from green tea induce apoptosis of tumor cell lines [26, 27]. In addition, PLCβ is known to be involved in cancer. It was reported that increased chemokines in the tumor microenvironment activate PLCβ through GPCRs and increase tumor cell migration and invasion [28]. The
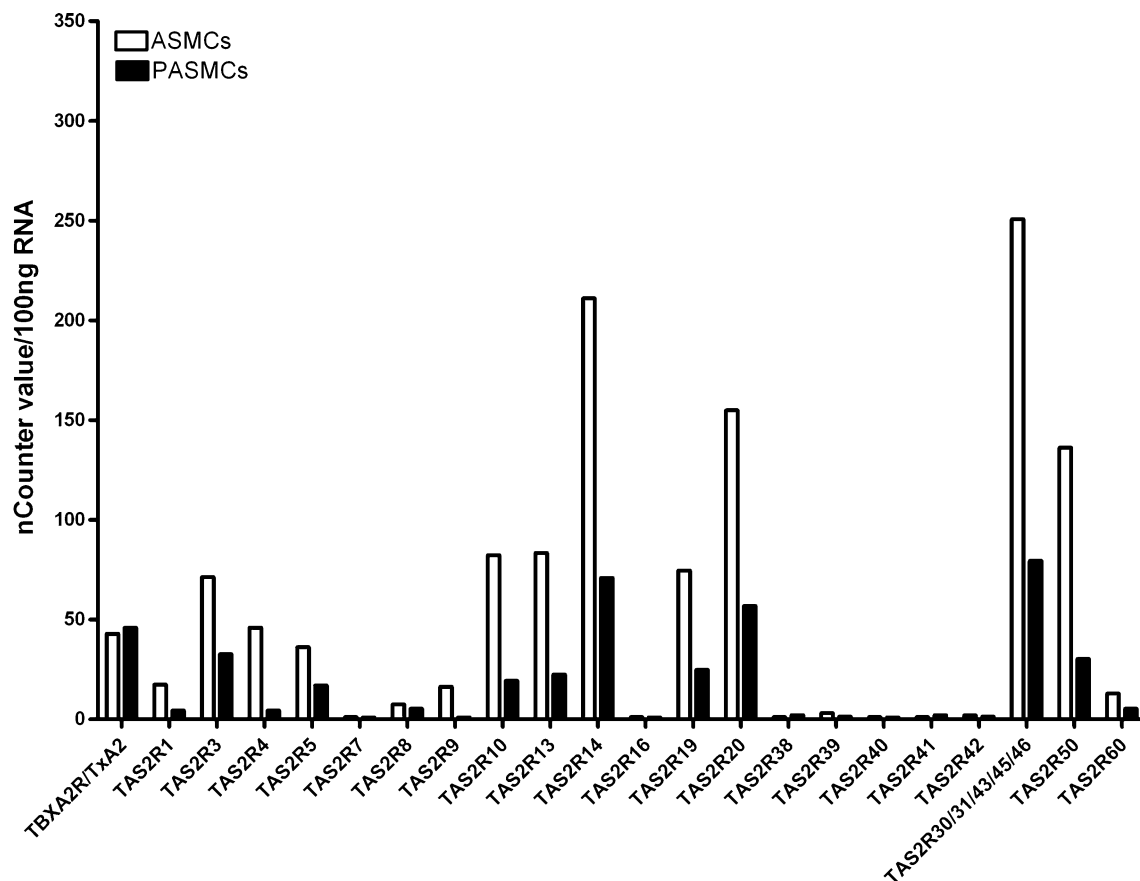
Fig. 3 The mRNA expression levels of TAS2Rs in hASMCs and hPASMCs. The nCounter analysis was performed as described in the "Methods" section. nCounter values were represented on the Y axis per 100 ng of RNA analyzed and the genes on the X axis. TBXA2R gene is included as a reference. Differential expression levels of TAS2Rs were observed in both cell lines, which is in agreement with previous studies

involvement of PLCβ in breast cancer invasion was also reported [29]. Our recent study suggests the differential expression of T2Rs in breast cancer cells [17]. Characterization of the expression and function of T2Rs in breast cancer might reveal their involvement in breast cancer invasion and apoptosis. This would aid in developing strategies to prevent and/or treat breast cancer.

To confirm the validity of the nCounter gene expression data, we analyzed the protein levels of select T2Rs in CuFi-1 and NuLi-1 airway cells by FACS. The main rationale for selecting these few T2Rs is based on the commercial availability of antibodies targeting the extracellular side of these T2Rs. The specificity of the antibody for the extracellular side is important, as it would allow the detection of T2Rs expressed on the cell surface, hence eliminating the need to permeabilize the cells. FACS analysis showed a similar protein expression trend as observed with the nCounter gene analysis, except for T2R4 (Fig. 4). The discrepancy in T2R4 expression at genetic and protein levels could be due to the polyclonal antibody used. It

should be noted that monoclonal antibodies for T2Rs are currently not available, and the approaches used to raise these different T2R polyclonal antibodies might vary.

Apart from studying the expression of T2Rs in different organs and tissues, it is important to study their functionality. In our previous studies, we showed that T2Rs expressed in brain, breast epithelium, and vasculature are functional [10, 16, 17]. Thus, in order to analyze whether the endogenous T2Rs expressed in bronchial epithelium are functional, we pursued calcium mobilization assays on NuLi-1 and CuFi-1 cells. We used the bitter compound quinine, which is known to activate multiple T2Rs [30]. These include T2R4, T2R7, T2R14, T2R39, T2R40, T2R43, T2R44, and T2R46 expressed in CuFi-1 and NuLi-1 cells (Fig. 1). Treatment of CuFi-1 and NuLi-1 cells with quinine caused a dose-dependent increase in intracellular calcium mobilization with EC_{50} values of 758 ± 77 and 925 ± 207 μM, respectively (Fig. 5a). This suggests that the T2Rs expressed in these cells are functional. However, no statistically significant change in the EC_{50} values was
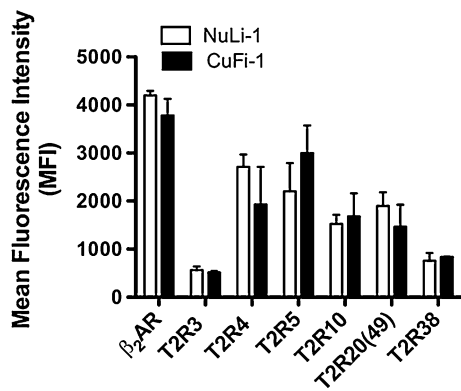
Fig. 4 Analysis of cell surface expression of endogenous T2Rs expressed in NuLi-1 and CuFi-1 cells by FACS. To confirm the expression of selected T2Rs at protein level, the cells were surface stained with polyclonal anti-T2R antibodies (1:200 or 1:300), monoclonal anti-β_2AR antibody (positive control), and the corresponding secondary antibody conjugated with Alexa Fluor-488 (1:1000). The data represent at least two independent experiments and the expression was presented as mean fluorescence intensity (MFI). To analyze the T2R-specific protein expression, the MFI values of isotype controls were subtracted. Two-way ANOVA with Bonferroni post hoc test was performed and no statistical significance was observed between CuFi-1 and NuLi-1 cells

observed for quinine treatment between the two cell lines, indicating that the disease-causing mutations may not influence the function of T2Rs in bronchial epithelium. T2Rs signal predominantly through the heterotrimeric G$\alpha\beta\gamma$ protein–phospholipase C (PLC)-dependent pathway leading to intracellular calcium mobilization. The PLC inhibitor, U-73122, inhibits the coupling of G$\alpha\beta\gamma$ protein–phospholipase C activation, making it a very useful tool to validate the

T2R–G$\alpha\beta\gamma$–PLC–Ca^{2+} pathway in these cells [9, 31, 32]. To further confirm that the above-observed functional response upon quinine treatment is through T2R signaling pathway, we treated NuLi-1 and CuLi-1 cells with U-73122 and measured their activation by quinine. Treatment with U-73122 caused a dramatic inhibition of quinine-mediated calcium response resulting in a right shift of the curves with EC$_{50}$ values of 2206 $\pm$ 23 and 1664 $\pm$ 59 μM observed for CuFi-1 and NuLi-1 cells, respectively (Fig. 5a, b). This suggests that majority of the intracellular calcium mobilization observed in these cells is due to the activation of T2Rs. To the best of our knowledge, this is the first study reporting the presence of functional T2Rs in the CF and non-CF bronchial epithelial cell lines.

Cell lines offer a unique and unparalleled advantage when trying to elucidate the role of novel cellular signal transduction pathways. Our results suggest a specific pattern of TAS2R expression with TAS2R3, 4, 5, 10, 13, 19, and 50 transcripts expressed at moderate levels and TAS2R14 and TAS2R20 (or 49) at high levels. The transcripts for the rest of the TAS2Rs are barely detectable or expressed at very low levels. Interestingly, TAS2R in non-cancerous vs. breast cancer cells shows differential expression which is not observed in other pathological cell lines analyzed. This study suggests the significant expression of a number of TAS2Rs in different tissues in both normal and pathophysiological conditions. The pathological environment in diseased conditions may regulate T2R functions and was recently reviewed elsewhere [5, 33]. Studies directed at understanding the functions of T2Rs in these extraoral tissues are much needed.
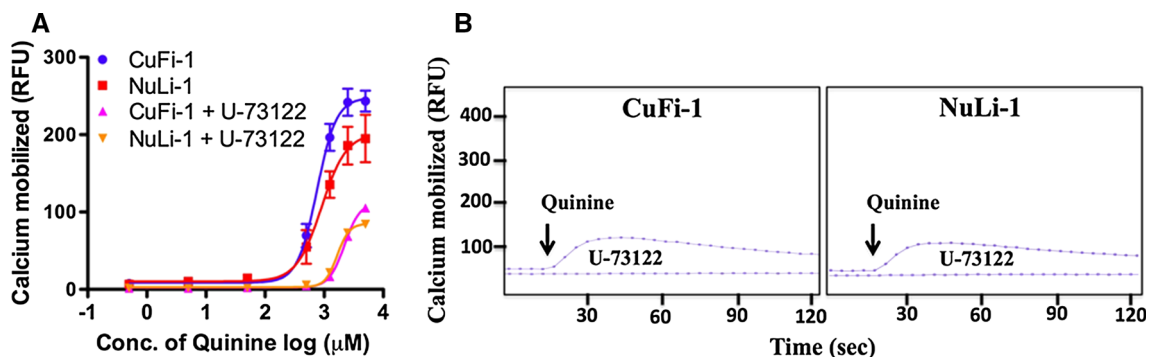

Fig. 5 Functional response of CuFi-1 and NuLi-1 cells to the bitter agonist quinine. **a** Concentration-dependent changes in intracellular calcium induced by the bitter compound quinine (70–5000 μM) in CuFi-1 and NuLi-1 cells and the same cells treated with the PLC inhibitor, U-73122 (5 μM for 30 min prior to quinine addition). Changes in intracellular calcium mobilized as detected by calcium-sensitive dye Fluo 4NW (Invitrogen) were measured in RFUs. Data represent four independent experiments with each data point in triplicate. For the measurement of dose–response curve, signals of 10–15 wells receiving the same concentrations of quinine were averaged. The EC$_{50}$ values for quinine in CuFi-1 and NuLi-1 cells are 758 $\pm$ 77 μM and 925 $\pm$ 207 μM, respectively. Treatment with PLC inhibitor, U-73122, as described in the "Methods" section caused a dramatic inhibition of quinine-mediated calcium response. EC$_{50}$ values and regression analysis were calculated using GraphPad Prism 5.0 software. **b** Representative calcium traces of untreated CuFi-1 and NuLi-1 cells, and cells treated with U-73122 (5 μM for 30 min prior to quinine addition) and stimulated with quinine (625 μM). *Arrows* indicate the time point (20 s) at which the bitter agonist quinine was added

References

1. Sharman JL, Benson HE, Pawson AJ, Lukito V, Mpamhanga CP, Bombail V, Davenport AP, Peters JA, Spedding M, Harmar AJ, Nc I (2013) IUPHAR-DB: updated database content and new features. Nucleic Acids Res 41(Database issue):D1083–D1088. doi:10.1093/nar/gks960

2. Adler E, Hoon MA, Mueller KL, Chandrashekar J, Ryba NJP, Zuker CS (2000) A novel family of mammalian taste receptors. Cell 100(6):693–702. doi:10.1016/S0092-8674(00)80705-9

3. Chandrashekar J, Mueller KL, Hoon MA, Adler E, Feng LX, Guo W, Zuker CS, Ryba NJP (2000) T2Rs function as bitter taste receptors. Cell 100(6):703–711. doi:10.1016/S0092-8674(00)80706-0

4. Wu SV, Rozengurt N, Yang M, Young SH, Sinnett-Smith J, Rozengurt E (2002) Expression of bitter taste receptors of the T2R family in the gastrointestinal tract and enteroendocrine STC-1 cells. Proc Natl Acad Sci USA 99(4):2392–2397. doi:10.1073/pnas.042617699

5. Shaik FA, Singh N, Arakawa M, Duan K, Bhullar RP, Chelikani P (2016) Bitter taste receptors: extraoral roles in pathophysiology. Int J Biochem Cell Biol. doi:10.1016/j.biocel.2016.03.011

6. Hofer D, Puschel B, Drenckhahn D (1996) Taste receptor-like cells in the rat gut identified by expression of alpha-gustducin. Proc Natl Acad Sci USA 93(13):6631–6634

7. Tizzano M, Gulbransen BD, Vandenbeuch A, Clapp TR, Herman JP, Sibhatu HM, Churchill MEA, Silver WL, Kinnamon SC, Finger TE (2010) Nasal chemosensory cells use bitter taste signaling to detect irritants and bacterial signals. Proc Natl Acad Sci USA 107(7):3210–3215. doi:10.1073/pnas.0911934107

8. Shah AS, Ben-Shahar Y, Moninger TO, Kline JN, Welsh MJ (2009) Motile cilia of human airway epithelia are chemosensory. Science 325(5944):1131–1134. doi:10.1126/science.1173869

9. Deshpande DA, Wang WC, McIlmoyle EL, Robinett KS, Schillinger RM, An SS, Sham JS, Liggett SB (2010) Bitter taste receptors on airway smooth muscle bronchodilate by localized calcium signaling and reverse obstruction. Nat Med 16(11):1299–1304. doi:10.1038/nm.2237

10. Upadhyaya JD, Singh N, Sikarwar AS, Chakraborty R, Pydi SP, Bhullar RP, Dakshinamurti S, Chelikani P (2014) Dextromethorphan mediated bitter taste receptor activation in the pulmonary circuit causes vasoconstriction. PLoS ONE 9(10):e110373. doi:10.1371/journal.pone.0110373

11. Foster SR, Porrello ER, Purdue B, Chan HW, Voigt A, Frenzel S, Hannan RD, Moritz KM, Simmons DG, Molenaar P, Roura E, Boehm U, Meyerhof W, Thomas WG (2013) Expression, regulation and putative nutrient-sensing function of taste GPCRs in the heart. PLoS ONE 8(5):e64579. doi:10.1371/journal.pone.0064579

12. Li F, Zhou ML (2012) Depletion of bitter taste transduction leads to massive spermatid loss in transgenic mice. Mol Hum Reprod 18(6):289–297. doi:10.1093/molehr/gas005

13. Clark AA, Dotson CD, Elson AE, Voigt A, Boehm U, Meyerhof W, Steinle NI, Munger SD (2015) TAS2R bitter taste receptors regulate thyroid function. FASEB J 29(1):164–172. doi:10.1096/fj.14-262246

14. Maurer S, Wabnitz GH, Kahle NA, Stegmaier S, Prior B, Giese T, Gaida MM, Samstag Y, Hansch GM (2015) Tasting *Pseudomonas aeruginosa* biofilms: human neutrophils express the bitter receptor T2R38 as sensor for the quorum sensing molecule N-(3-oxododecanoyl)-l-homoserine lactone. Front Immunol 6:369. doi:10.3389/fimmu.2015.00369

15. Wolfle U, Elsholz FA, Kersten A, Haarhaus B, Muller WE, Schempp CM (2015) Expression and functional activity of the bitter taste receptors TAS2R1 and TAS2R38 in human keratinocytes. Skin Pharmacol Physiol 28(3):137–146. doi:10.1159/000367631

16. Singh N, Vrontakis M, Parkinson F, Chelikani P (2011) Functional bitter taste receptors are expressed in brain cells. Biochem Biophys Res Commun 406(1):146–151. doi:10.1016/j.bbrc.2011.02.016

17. Singh N, Chakraborty R, Bhullar RP, Chelikani P (2014) Differential expression of bitter taste receptors in non-cancerous breast epithelial and breast cancer cells. Biochem Biophys Res Commun 446(2):499–503. doi:10.1016/j.bbrc.2014.02.140

18. Lund TC, Kobs AJ, Kramer A, Nyquist M, Kuroki MT, Osborn J, Lidke DS, Low-Nam ST, Blazar BR, Tolar J (2013) Bone marrow stromal and vascular smooth muscle cells have chemosensory capacity via bitter taste receptor expression. PLoS ONE 8(3):e58945. doi:10.1371/journal.pone.0058945

19. Foster SR, Roura E, Thomas WG (2014) Extrasensory perception: odorant and taste receptors beyond the nose and mouth. Pharmacol Ther 142(1):41–61. doi:10.1016/j.pharmthera.2013.11.004

20. Kulkarni M (2011) Digital multiplexed gene expression analysis using the NanoString nCounter system. Curr Protoc Mol Biol/edited by Frederick M Ausubel[et al]:Unit25B. 10

21. Geiss GK, Bumgarner RE, Birditt B, Dahl T, Dowidar N, Dunaway DL, Fell HP, Ferree S, George RD, Grogan T, James JJ, Maysuria M, Mitton JD, Oliveri P, Osborn JL, Peng T, Ratcliffe AL, Webster PJ, Davidson EH, Hood L, Dimitrov K (2008) Direct multiplexed measurement of gene expression with color-coded probe pairs. Nat Biotechnol 26(3):317–325. doi:10.1038/nbt1385

22. Liggett SB (2013) Bitter taste receptors on airway smooth muscle as targets for novel bronchodilators. Expert Opin Ther Targets 17(6):721–731. doi:10.1517/14728222.2013.782395

23. Foster SR, Porrello ER, Stefani M, Smith NJ, Molenaar P, Dos Remedios CG, Thomas WG, Ramialison M (2015) Cardiac gene expression data and in silico analysis provide novel insights into human and mouse taste receptor gene regulation. Naunyn-Schmiedeberg's Arch Pharmacol 388(10):1009–1027. doi:10.1007/s00210-015-1118-1

24. Robinett KS, Koziol-White CJ, Akoluk A, An SS, Panettieri RA Jr, Liggett SB (2014) Bitter taste receptor function in asthmatic and nonasthmatic human airway smooth muscle cells. Am J Respir Cell Mol Biol 50(4):678–683. doi:10.1165/rcmb.2013-0439RC

25. Bravi F, Bosetti C, Tavani A, Gallus S, LaVecchia C (2013) Coffee reduces risk for hepatocellular carcinoma: an updated meta-analysis. Clin Gastroenterol Hepatol 11(11):1413. doi:10.1016/j.cgh.2013.04.039

26. Gao F, Li M, Liu WB, Zhou ZS, Zhang R, Li JL, Zhou KC (2015) Epigallocatechin gallate inhibits human tongue carcinoma cells via HK2-mediated glycolysis. Oncol Rep 33(3):1533–1539. doi:10.3892/or.2015.3727

27. Lamy V, Roussi S, Chaabi M, Gosse F, Schall N, Lobstein A, Raul F (2007) Chemopreventive effects of lupulone, a hop beta-acid, on human colon cancer-derived metastatic SW620 cells and

in a rat model of colon carcinogenesis. Carcinogenesis 28(7):1575–1581. doi:10.1093/carcin/bgm080

28. Park JB, Lee CS, Jang JH, Ghim J, Kim YJ, You S, Hwang D, Suh PG, Ryu SH (2012) Phospholipase signalling networks in cancer. Nat Rev Cancer 12(11):782–792. doi:10.1038/nrc3379

29. Bertagnolo V, Benedusi M, Brugnoli F, Lanuti P, Marchisio M, Querzoli P, Capitani S (2007) Phospholipase C-beta 2 promotes mitosis and migration of human breast cancer-derived cells. Carcinogenesis 28(8):1638–1645. doi:10.1093/carcin/bgm078

30. Upadhyaya JD, Chakraborty R, Shaik FA, Jaggupilli A, Bhullar RP, Chelikani P (2016) The pharmacochaperone activity of quinine on bitter taste receptors. PLoS ONE 11(5):e0156347. doi:10.1371/journal.pone.0156347

31. Zhang CH, Lifshitz LM, Uy KF, Ikebe M, Fogarty KE, ZhuGe R (2013) The cellular and molecular basis of bitter tastant-induced bronchodilation. PLoS Biol 11(3):e1001501. doi:10.1371/journal.pbio.1001501

32. Pydi SP, Singh N, Upadhyaya J, Bhullar RP, Chelikani P (2014) The third intracellular loop plays a critical role in bitter taste receptor activation. BBA Biomembr 1838(1):231–236. doi:10.1016/j.bbamem.2013.08.009

33. Pydi SP, Upadhyaya JD, Singh N, Bhullar RP, Chelikani P (2012) Recent advances in structure and function studies of bitter taste receptors. Curr Protein Pept Sci 13(6):501–508